Chemical Engineering Journal 93 (2003) 163–172

Chemical Engineering Journal

www.elsevier.com/locate/cej

Equilibrium and kinetics properties of *p*-dichlorobenzene and toluene on silica gel in dense CO_2 by chromatography analysis

Xiaoning Yang [a,*], Michael A. Matthews [b]

[a] *College of Chemistry and Chemical Engineering, Nanjing University of Technology, Nanjing 210009, PR China*
[b] *Department of Chemical Engineering, University of South Carolina, Columbia, SC 29208, USA*

Abstract

The adsorption equilibrium constant and kinetics properties for *p*-dichlorobenzene and toluene on silica gel adsorbent in the subcritical and supercritical CO_2 have been measured by an impulse chromatography technique. The experiments were performed at temperatures of 298.15, 208.15, 318.15 K and pressures of 75–178 bar. A series fit method was applied to treat the chromatography peak. The adsorption equilibrium constant increased with temperature and decreased with pressure under the experimental conditions. The fluid density is found to be the main controlling factor determining the adsorption equilibrium constant. The dependence of the kinetics properties, dispersion coefficient and intraparticle effective diffusivity, on temperature and pressure has been investigated. The pore diffusion is the main diffusion mechanism within the pore medium. The partial molar volume (PMV) and partial molar enthalpy (PME) for *p*-dichlorobenzene in supercritical CO_2 have also been evaluated from the adsorption equilibrium constants obtained in this work. Very large and negative values for the two partial molar properties were obtained near the critical point of CO_2.

Keywords: Chromatography; Kinetic properties; Supercritical fluid chromatography; Partial molar volume

1. Introduction

Supercritical CO_2 fluid has received widespread attention in different industrial and environmental cleaning processes [1]. Besides its environmentally benign nature, two groups of properties make the supercritical fluid an attractive solvent: First, its adaptable thermodynamics properties (liquid-like density), secondly a lower viscosity and a higher diffusion property, which are favorable in practical processes [2]. The use of the supercritical CO_2 fluid involving solid materials includes extraction of natural organic compound from plants, decontamination of environmental solids, regeneration of adsorbents and catalysts, adsorptive separation and heterogeneous catalytic reactions in supercritical environmental medium. Adsorption equilibrium and mass transfer at the fluid–solid interface may play a key role in all these processes [3]. For example, in extraction from solid matrices, the adsorption equilibrium of solute in supercritical CO_2 determines the thermodynamic extent of the extraction, and the mass transfer parameters, such as axial dispersion coefficient and effective intraparticle diffusivity, control the process rate, which is very important in designing industrial extractors.

Supercritical fluid chromatography (SFC) is an effective method that has been applied in compound analysis, preparative scale separation as well as physicochemical property measurement [1]. Due to the existing complexity and difficulty in physicochemical property measurement and estimation under supercritical state, the supercritical fluid chromatography deserves a special interest in studying the adsorption equilibrium and mass transfer within a solid media under supercritical conditions. The foundation of determining the physicochemical properties using supercritical fluid chromatography is based on the theory of chromatography [4,5]. In some previous works, Shim and Johnston [6] determined a variety of thermodynamic properties at infinite dilution using SFC, and Erkey and Akgerman [7] applied a chromatographic tracer response technique to determine the adsorption equilibrium and mass transfer properties for naphthalene on alumina in supercritical CO_2.

In this study, the adsorption equilibrium and mass transfer properties of 1,4-dichlorobenzene and toluene on the silica gel in the dense CO_2 were evaluated and investigated by SFC. Toluene is an important solvent used in the chemical industry. Its recovery by supercritical CO_2 is a promising method. Also 1,4-dichlorobenzene is possibly carcinogenic to humans and is of environmental concern. We have measured the adsorption equilibrium constants

* Corresponding author.
E-mail address: yangxia@njuct.edu.cn (X. Yang).

1385-8947/02/$ – see front matter
PII: S1385-8947(02)00254-1

Nomenclature

D_e	intraparticle effective diffusivity (m^2/s)
D_m	bulk diffusion coefficient (m^2/s)
d_p	solid particle diameter (m)
D_{ax}	axial dispersion coefficient (m^2/s)
h	partial molar enthalpy (kJ/mol)
k_{ad}	adsorption rate constant ($cm^3/g\,s$)
k_f	film mass transfer coefficient (m/s)
K_2	adsorption equilibrium constant (cm^3/g)
L	length of the packed bed (m)
n_p	number of experimental points
P	system pressure (bar)
r	particle radius (m)
R	gas constant (J/mol K)
t	time (s)
t_R	retention time (s)
T	system temperature (K)
u	interstitial velocity (m/s)
V_i^∞	partial molar volume of solute i (cm^3/mol)

Greek letter

α	volume expansivity of fluid (K^{-1})
β	volume compressibility of fluid (bar^{-1})
ε_p	void fraction of particle
ε_b	void fraction of bed
η	viscosity of fluid (Pa s)
λ	ratio of molecular diameter to pore diameter of particle
ρ	density of fluid (g/cm^3)
ρ_p	particle density (g/cm^3)
τ	tortuosity factor

for the two solutes in dense CO_2, and their partial molar properties at infinite dilution in CO_2 were estimated. The axial dispersion coefficient and the effective intraparticle diffusivity were also studied.

2. Theoretical background

The impulse response in a packed column is governed by a system of coupled partial differential equations, in which the equilibrium adsorption mechanism and mass transfer processes, including intraparticle diffusion, external fluid–particle mass transfer, and axial dispersion, are considered [5,8]. As the solute concentration in dense CO_2 is very dilute for the systems, it is reasonable that the adsorption isotherm is assumed to be linear. The average retention time t_R and the variance σ^2 of the response curve for the systems are expressed as:

$$t_R = \frac{L}{u}(1+\delta_0) \tag{1}$$

$$\sigma^2 = \frac{2L}{u}(\delta_{ax}+\delta_f+\delta_d+\delta_{ad}) \tag{2}$$

where

$$\delta_0 = \frac{1-\varepsilon_b}{\varepsilon_b}(\varepsilon_p+\rho_p K_2) \tag{3}$$

$$\delta_{ax} = \frac{D_{ax}}{u^2}(1+\delta_0)^2 \tag{4}$$

$$\delta_f = \frac{1-\varepsilon_b}{\varepsilon_b}\frac{r}{3k_f}(\varepsilon_p+\rho_p K_2)^2 \tag{5}$$

$$\delta_d = \frac{1-\varepsilon_b}{\varepsilon_b}\frac{r^2}{15D_e}(\varepsilon_p+\rho_p K_2)^2 \tag{6}$$

$$\delta_{ad} = \frac{1-\varepsilon_b}{\varepsilon_b}\frac{\rho_p K_2^2}{k_{ad}} \tag{7}$$

where K_2 is the solute adsorption equilibrium constant. For mass transfer parameters, D_{ax} is the axial dispersion coefficient, D_e the intraparticle effective diffusivity, k_f the external fluid film mass-transfer coefficient, and k_{ad} the adsorption rate constant. According to Eq. (1), a plot of t_R versus L/u should be a straight line through the origin. The adsorption equilibrium constant K_2 can be estimated from the slope of the straight line.

For kinetics properties, Eq. (2) can be rearranged into

$$\frac{\delta^2}{2t_R} = \frac{D_{ax}}{u^2}(1+\delta_0)+\frac{\delta_1}{1+\delta_0} \tag{8}$$

where $\delta_1 = \delta_{ad}+\delta_f+\delta_d$. In this following analysis, the adsorption rate constant, k_{ad}, was assumed to be infinitely large because the adsorption rate is usually very fast [9]. The external mass transfer coefficient, k_f, may be estimated by a correlation equation in literatures. As D_{ax}/u can be considered to be constant at low Reynolds number in packed beds [10], a plot of $\sigma^2/2t_R$ against $1/u$ may give a straight line with an intercept of $\delta_1/(1+\delta_0)$ and a slope of $D_{ax}(1+\delta_0)/u$. Thus, the axial dispersion coefficient, D_{ax}, and the intraparticle effective diffusivity, D_e, can be evaluated from the slope and the intercept, respectively.

The average retention time t_R characterizes the position of the center of gravity of the response peak and whereas the variance σ^2 characterizes the width of the peak. They are given in the following definition:

$$t_R = \frac{\int_0^\infty tV(L,t)\,dt}{\int_0^\infty V(L,t)\,dt} \tag{9}$$

$$\sigma^2 = \frac{\int_0^\infty (t-t_R)^2 V(L,t)\,dt}{\int_0^\infty V(L,t)\,dt} \tag{10}$$

where $V(L, t)$ is the detected signal versus time at the exit of the adsorption column. In practice, most of the numerical integrations required for calculation t_R and σ^2 are carried out over finite limits and depend very heavily on the experimental baseline and response curve shape. In the Eq. (10), due to the $(t-t_R)^2$ weighting, a significant variation may

be caused in the calculation of the second or higher moment when the integration limit are extended to include more baseline points.

In order to eliminate this drawback, an alternative method based on series fit to experimental response peaks has been applied in the determination of the retention time and the variance of the response curve. Different analytical forms are reported in the curve fitting of the chromatographic peaks [11]. Among these, the Edgeworth–Cramer (EC) series is of particular interest because it is generally developed with the parameters of mathematical statistical meaning [12]. Also this series has the advantage that it is able to fit very skewed peaks [12]. The EC series expression can be written in the form [11–13],

$$V(t) = \frac{A}{\sigma}\left[f(x) - \frac{s}{3!}f^{(3)}(x) + \frac{e}{4!}f^{(4)}(x) - \frac{q}{5!}f^{(5)}(x) + \frac{10s^2}{6!}f^{(6)}(x) - \frac{35se}{7!}f^{(7)}(x) - \frac{280s^3}{9!}f^{(9)}(x) + \cdots\right] \quad (11)$$

where $f(x)$ is the normalized Gaussian function and it is given in the form

$$f(x) = \frac{1}{\sqrt{2\pi}}\exp\left(-\frac{x^2}{2}\right) \quad (12)$$

with

$$x = \frac{t - t_R}{\sigma}$$

$f^{(v)}(x)$ is the vth derivative of the normal Gaussian function $f(x)$, and it can be obtained from successive Hermite polynomials as follows.

$$f^{(v)}(x) = \left(\frac{-1}{\sqrt{2}}\right)^{(v)} H_v\left(\frac{x}{\sqrt{2}}\right) f(x) \quad (13)$$

where $H_v(x)$ is the vth Hermite polynomial [13]. The parameter s is the skewness, e is excess, and q is the unnamed parameter. They are related respectively to the third, the fourth, and the fifth moments of the peak. Therefore, there are six parameters, the retention time t_R, the variance σ^2, the peak area A, together with s, e, and q, to be determined by the fitting of peak curve. This method may provide some additional information on the higher moments of the peak. We use a nonlinear least technique to obtain these parameters. The minimized function is

$$\mathrm{FCN} = \sum_{1}^{n_p}[V(t, L)_{exp} - V(t, L)_{ES}]^2 \quad (14)$$

where $V(t, L)_{exp}$ is the experimental data from the UV detector, and $V(t, L)_{ES}$ the values of the ES series.

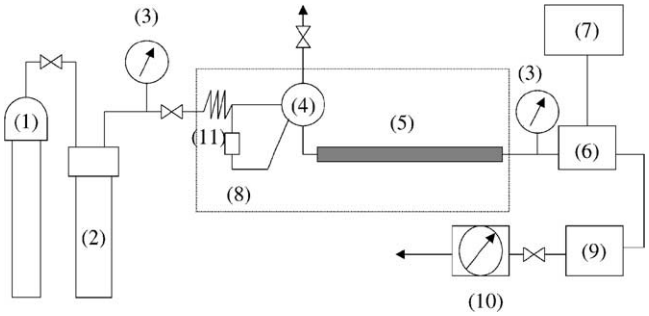

Fig. 1. Schematic diagram of the experimental apparatus.

3. Experimental

3.1. Apparatus

A schematic of the experimental apparatus is shown in Fig. 1. Zero dead volume fittings were used throughout the apparatus. Dense CO_2, which was a solvent as well as a carrier gas, was compressed by a pulse-less micro-pump (ISCO, μLC-500) and was pumped into the system. The pump head was kept cooler by a cooling unit that ensured that liquid CO_2 was available at the pump exit. We used a backpressure regulator charged with nitrogen to control the system pressure, which is monitored by using a high accuracy (0.01%) digital pressure transducer (DIGIQUARTZ PAROSCIENTIFIC, model 740). A manual high-pressure generator (High Pressure Equipment, model 62-6-10) was used to compress the nitrogen gas for the backpressure regulator, with which the pressure control can be made easily. The pressure drop across the adsorption was <0.4 bar through all experimental conditions. The adsorption column is made of stainless steel and the tube fittings with frits are used to prevent column end effects. The characteristics of the adsorption column are given in Table 1. The sample was prepared by passing CO_2 carried gas through a cell containing the solutes. The sample was injected into the adsorption column through a high pressure injection valve (Valco, model A60, equipped with 10–15 μl sample loop) with helium-drive gas actuator. A model WB1130 (LINDBERG/BLUE) constant temperature water bath is used to maintain the system temperature. The effluent, i.e. the concentration at the outlet of the adsorption column, was detected by a UV variable wavelength HPLC

Table 1
Characteristics of the packed bed and the silica gel

Bed length	0.242 m
Bed diameter	0.00380 m
Bed porosity	0.420
Particle diameter	3.35×10^{-4} m
Particle porosity	0.475
Particle density	0.801 g/cm^3
Specific surface area	500 m^2/g
Mean pore diameter	60 Å

detector (LINEAR, model 200). A capillary tube is used as the sample cell for the UV detector, and this arrangement eliminates any peak broadening due to the finite volume of the flow-cell in the previous UV detector. The UV detector signal was captured by a computer with a data acquisition system. The volume flow rate of the CO_2 carrier fluid was measured by a wet gas meter.

3.2. Materials

Silica gel (Alltech, grade 40–60) was packed in the adsorption column as the solid adsorption particle. The characteristics of the packed bed and the packed solid particle are given in Table 1. The particles were first sieved and washed with distilled water to remove the fines. The solid particles were dried over 24 h before use. High purity carbon dioxide (99.9%) was used as a carrier gas. Reagent-grade toluene (Fisher, 99.8%) and 1,4-dichlorobenzene (Aldrich, >99%) were used as received without further purification in this work.

4. Results and discussions

4.1. Evaluation of the series fitting

Many previous researches have proven that the EC series is very effective to determine the parameters with statistical meanings for the chromatographic peaks, even for very skewed peaks [11]. Fig. 2 gives typical fitting results for response curves in this study together with the major parameters in the EC series. An excellent agreement is obtained between the experimental and fitting values for response peaks. Because of using similar flow rates, the difference in the retention times and the variances for the three peaks are caused by the pressure variation.

4.2. Adsorption equilibrium constants

Fig. 3 shows the plots of t_R versus L/u obtained from the chromatographic peaks for 1,4-dichlorobenzene/CO_2 system at the three temperatures. Fairly good linearity passing through the origin of the plots was obtained at all experimental conditions. Fig. 4 gives similar results for toluene/CO_2 system. All the lines shown in these figures were obtained from the least square analysis with the linearity correlation coefficients in all cases above 0.999. The observed linearity in Figs. 3 and 4 confirmed that the model development is reasonable. The assumption that the adsorption equilibrium of the two solutes in the silica gel/CO_2 system is linear is proven to be correct.

The adsorption equilibrium constants (K_2) were evaluated from the slopes of the linear plots and are given in Table 2. It seems that the difference in K_2 between the two solutes is not very obvious. This means that the adsorption affinity

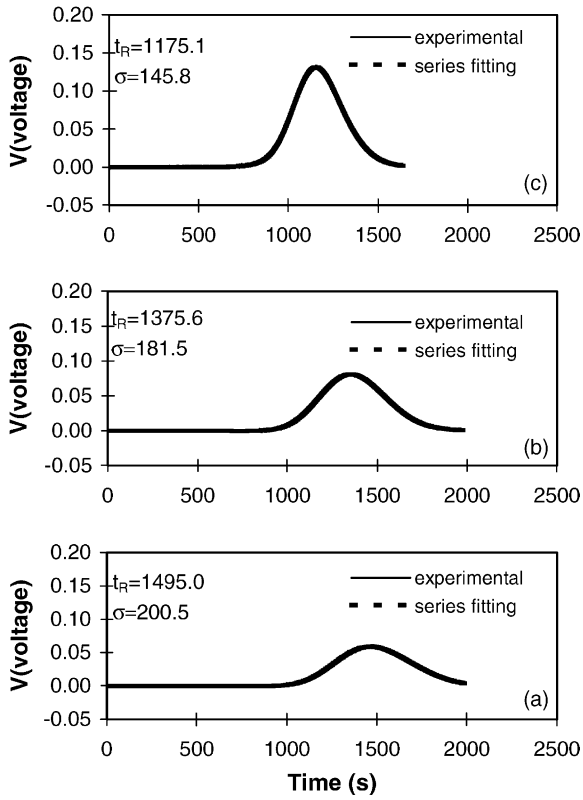

Fig. 2. A typical response peak for toluene at 308.15 K with the same flow rate and different pressures: (a) 107.9 bar; (b) 142.4 bar; (c) 197.5 bar.

of the two solutes onto the silica gel in the dense CO_2 is almost equivalent. Fig. 5 shows the relation of the adsorption equilibrium constant (K_2) with pressure. K_2 decreases with an increase in pressure at constant temperature. This behavior is similar with the results by Erkey and Akgerman

Table 2
Adsorption equilibrium constants of two solutes in silica gel/CO_2

T (K)	P (bar)	ρ (g/cm^3)	K_2 (cm^3/g)
1,4-Dichlorobenzene			
298.15	74.46	0.7600	2.648
	107.9	0.8299	1.899
	142.4	0.8699	1.578
	176.9	0.8988	1.422
308.15	82.74	0.5697	5.286
	107.9	0.7390	2.810
	142.4	0.8054	1.946
	174.8	0.8434	1.626
318.15	107.9	0.5888	5.429
	142.4	0.7270	2.819
	174.8	0.7829	2.127
Toluene			
308.15	107.9	0.7390	2.938
	142.4	0.8054	2.137
	174.4	0.8431	1.805
	197.5	0.8641	1.421
318.15	107.9	0.5889	5.300
	142.4	0.7270	3.026
	174.8	0.7829	2.473

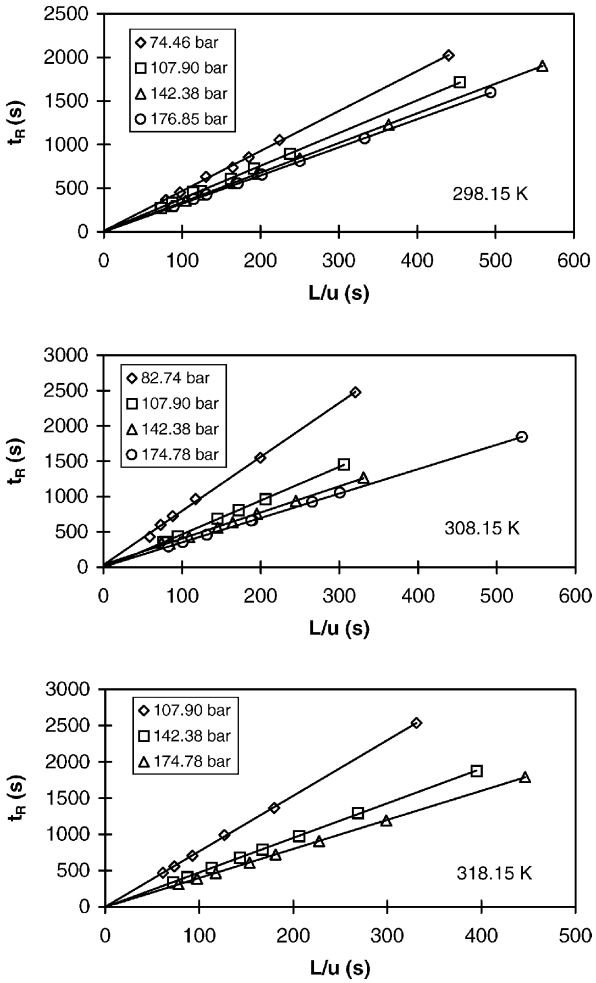

Fig. 3. Relation of the retention time (t_R) with L/u for 1,4-dichlorobenzene.

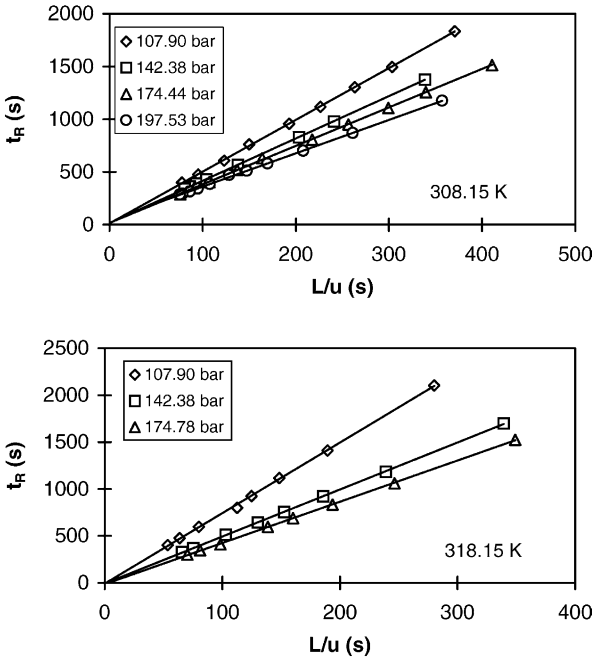

Fig. 4. Relation of the retention time (t_R) with L/u for toluene.

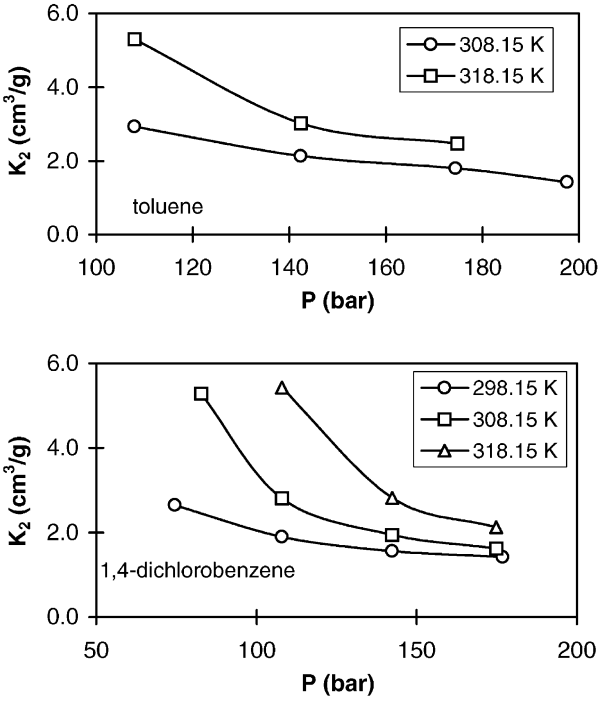

Fig. 5. Dependence of adsorption equilibrium constant on pressure.

[7] and Lee et al. [14]. This can be explained as the cause that the solvating power of CO_2 increases with pressure. Another reason is the competitive adsorption of CO_2 [15], which may also contribute to an isothermal reduction of K_2 with pressure.

According to Fig. 5, the adsorption equilibrium constant (K_2) increases with temperature at constant pressure in the experimental conditions. At fixed pressure, increasing temperature will lead to two opposite factors. For example, adsorption will increase with temperature due to an exothermic effect, but increasing temperature will cause a decrease in fluid density, thus it may enhance the adsorption because of the reduction of the solvating power of fluid [6,14]. The actual behavior of K_2 is dependent on a major contribution (or a controlling factor). The isobaric temperature dependence of the adsorption equilibrium shows that the controlling factor is the fluid density.

The isochoric temperature dependence is relatively insignificant from the subcritical to supercritical conditions in this work as shown in Fig. 6, which is similar to those obtained by Sato et al. [16] and Goto et al. [17]. The fluid densities of CO_2 were calculated from an equation of state of CO_2 [18]. This experimental result confirms again that the controlling factor for the adsorption equilibrium constant in the experimental conditions is the fluid density.

4.3. Partial molar volume and partial molar enthalpy of 1,4-dichlorobenzene

Partial molar properties of solutes at infinite dilution in the supercritical fluid are very important parameters for

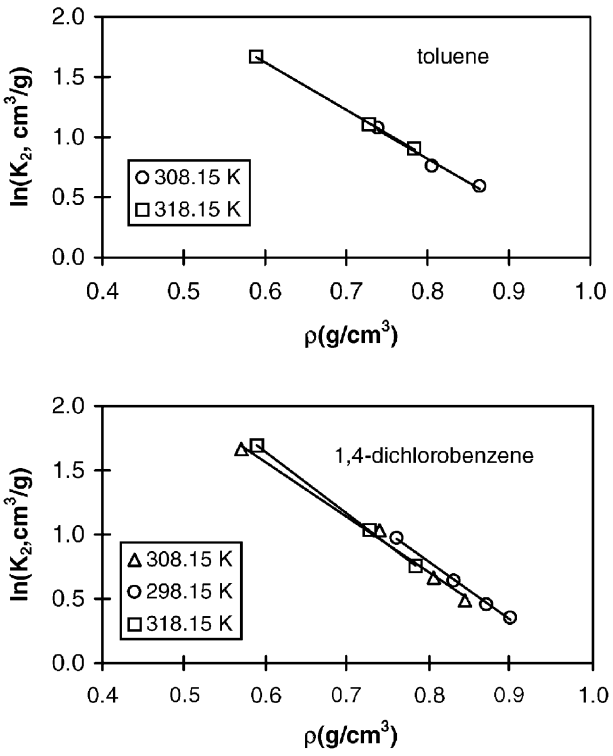

Fig. 6. Dependence of adsorption equilibrium constant on fluid density.

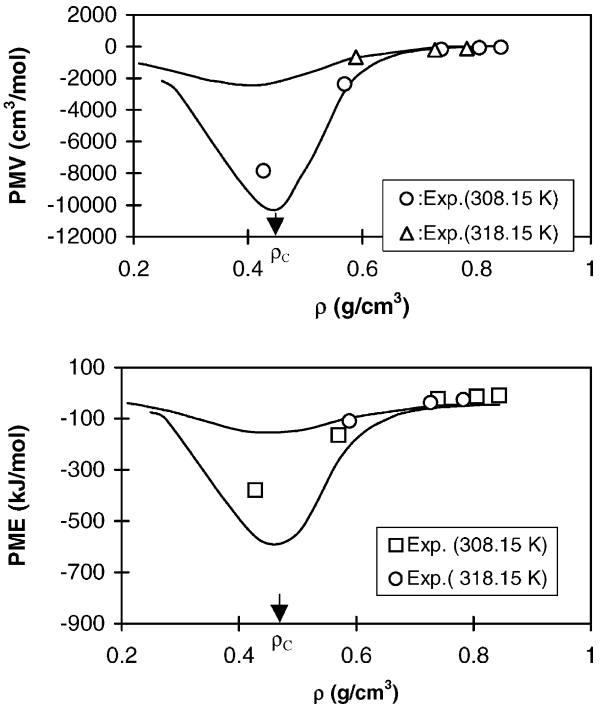

Fig. 7. Partial molar properties of 1,4-dichlorobenzene at infinite dilution: (solid line) from PR equation of state; (symbol) from the adsorption equilibrium constant.

understanding molecular interactions [19]. The partial molar volume (PMV) of solutes at infinite dilution can be calculated by the adsorption equilibrium constant [6,20].

$$V_2^{\infty} = RT\beta\left[1 + \rho\left(\frac{\partial(\ln K_2)}{\partial\rho}\right)_T\right] \quad (15)$$

where $\beta(-(1/V)(\partial V/\partial P)_T)$ is the isothermal compressibility. Eq. (15) was derived by eliminating the partial molar volume of solute in the adsorbed phase [6]. In the vicinity of the critical point, where larger negative value of the partial molar volume was observed as seen in the next passage, while the contribution of the partial molar volume of solute on the adsorbent is relatively small, therefore, Eq. (15) is applicable to estimate the partial molar volumes near the critical point.

The partial molar volumes of 1,4-dichlorobenzene calculated by Eq. (15) are shown in Fig. 7, where the isothermal compressibility was obtained from the equation of state of CO_2 [18]. In the use of Eq. (15), the relation of $\ln K_2$ versus ρ was regressed very accurately with a polynomial in order to calculate $(\partial(\ln K_2)/\partial\rho)_T$. Due to unavailability of the experimental PMV, we have applied the PR equation of state [21] to evaluate the PMV of 1,4-dichlorobenzene in the supercritical CO_2 in order to compare with the values obtained from the adsorption equilibrium constant. In this calculation of PMV from the equation of state, the binary interaction parameter k_{12} is needed and is usually obtained by adjusting the experimental solubility data of solute in the supercritical CO_2. For 1,4-dichlorobenzene, no experimental solubility data is available, so we used the interaction parameter of its isomer, 1,2-dichlorobenzene, with k_{12} being 0.1275 [22].

As expected, very large and negative values for the partial molar volumes were obtained from the two methods. The large negative partial molar volumes are explained by the local density enhancement due to solvent molecules around solutes [23]. In Fig. 7, the PMV obtained from K_2 agree qualitatively with the values from PR equation of state. It is likely that the difference is due to the limitations of the equation of state in the accurate description of the partial molar volume very near the critical point. The chromatographic method can provide a fast and effective alternative to estimate the partial molar volume.

An analogous derivation is obtained for the partial molar enthalpy (PME) for solute at infinite dilution [20,24],

$$h_2^{\mathrm{F}} - h_2^{\mathrm{IG}} = h_2^{\mathrm{S}} - h_2^{\mathrm{IG}} - RT^2\left[\left(\frac{\partial(\ln K_2)}{\partial T}\right)_P - \alpha\right] \quad (16)$$

where α, $(1/V)(\partial V/\partial T)_P$, is the volume expansivity, and the superscripts IG, F, S represent the ideal gas state, mobile phase and solid phase, respectively.

The complex behavior of $(\partial(\ln K_2)/\partial T)_P$ can be expressed with the following relation,

$$\left(\frac{\partial(\ln K_2)}{\partial T}\right)_P = \left(\frac{\partial(\ln K_2)}{\partial T}\right)_\rho + \left(\frac{\partial(\ln K_2)}{\partial\rho}\right)_T \left(\frac{\partial\rho}{\partial T}\right)_P \quad (17)$$

Substitution of Eq. (17) into Eq. (16) yields,

$$h_2^{\mathrm{F}} - h_2^{\mathrm{IG}} = h_2^{\mathrm{S}} - h_2^{\mathrm{IG}} - RT^2\left(\frac{\partial(\ln K_2)}{\partial T}\right)_{\rho} + \alpha RT^2\left[1+\rho\left(\frac{\partial(\ln K_2)}{\partial \rho}\right)_T\right] \quad (18)$$

where $h_2^{\mathrm{S}} - h_2^{\mathrm{IG}}$ may be approximately replaced by the negative value of the vaporized heat [6], which is obtained from an estimating method [25]. In this study, the dependence of the adsorption equilibrium constant on temperature under a fixed density is relatively small, we assumed $(\partial(\ln K_2)/\partial T)_{\rho} \approx 0$. Since the two derivatives in Eq. (18) are relative constant, the modification of Eq. (18) will make the evaluation of PME easier. In Fig. 7, the calculated values of PME from K_2 under supercritical conditions together with the values from the PR equation of state were shown for 1,4-dichlorobenzene. A similar behavior as partial molar volume, with large and negative values, was observed near the critical point for partial molar enthalpy, as seen in Fig. 7. This suggests that the clustering interaction by solvent molecules around the solute molecule lead to a very large exothermic effect.

4.4. Mass transfer properties

Figs. 8 and 9 show the results of the second moments based on Eq. (8) The data points were a little scattered as compared with the first moment results. However, most plots show reasonable straight lines with correlation coefficients from 0.9861 to 0.9953, except 0.9488 at 308.15 K and 82.74 bar. The straight lines show that the theoretical model reasonably describes the mass transfer process occurring in the systems.

4.5. Axial dispersion coefficient

Axial dispersion in a packed bed has been extensively investigated for gases and liquids, though it is specific to the experimental conditions, such as geometry and flow regime. However, for supercritical fluids, only limited studies are reported [10,26,27]. In this work, we evaluated the dispersion coefficient from subcritical to supercritical conditions, and compared our values with the previous results. The D_{ax}/u ratios were calculated from the slopes of the plots in Figs. 8 and 9. The Peclet numbers, $Pe = du/D_{\mathrm{ax}}$, at the experimental conditions can be obtained. From Table 3 the Peclet numbers ranged from 0.17 to 0.26. The results in this study are lower than those by Tan and Liou [10], which lie from 0.60 to 2.7. However, the Peclet numbers obtained by Erkey and Akgerman [28] ranged from 0.058 to 0.247 for naphthalene in alumina/CO_2 systems, 0.08–0.39 for ethyl acetate in activated carbon/CO_2 [17] and 0.013–0.257 for limonene and linalool in supercritical CO_2 with silica gel adsorbent [16]. These previous results are consistent with our values. The

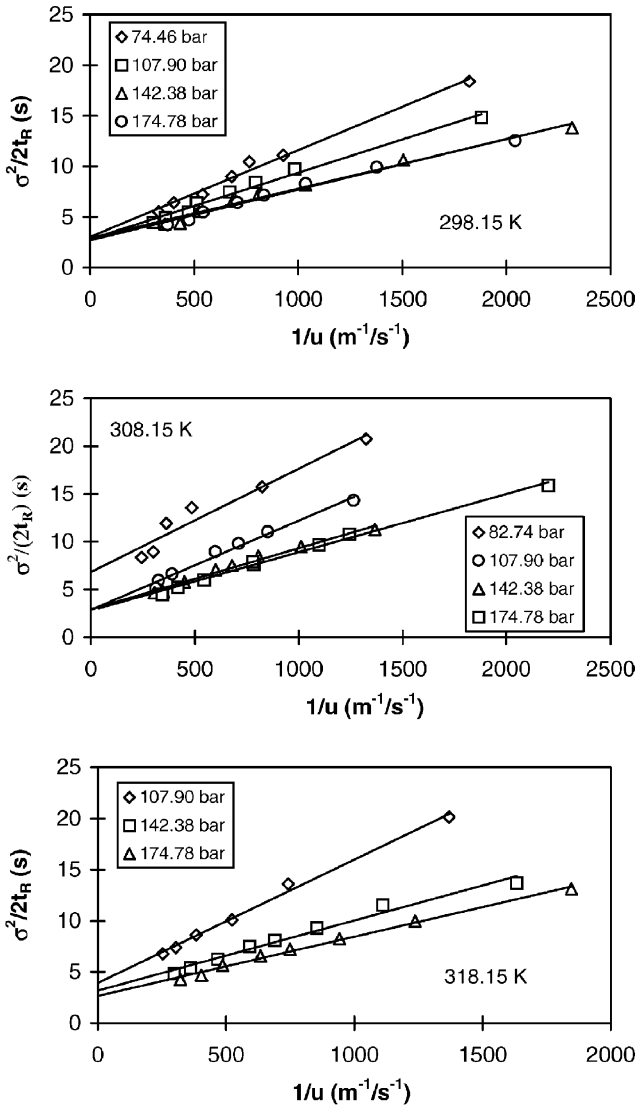

Fig. 8. Relation of $\sigma^2/2t_{\mathrm{R}}$ with the reciprocal velocity ($1/u$) for 1,4-dichlorobenzene.

observed relation between the Peclet and Reynolds numbers is shown in Fig. 10. By comparing with the previous correlation equations [26,27], the range of the Peclet numbers obtained in this study lies between those from the two correlation equations.

It is reported that the Peclet numbers are usually <1.0 for liquid and larger than 2.0 for gas [29,30]. The present experimental data for Pe show that the dispersion characteristic of the solutes in dense CO_2 is consistent with the behavior of liquid. For gas and liquid, the increase of axial dispersion with flow rate was observed [31,32]. The research by Tan and Liou [10] has found that the axial dispersion coefficients increase linearly with the interstitial velocity under certain conditions for supercritical fluid. The assumption that D_{ax}/u was constant for low Reynolds numbers in packed beds is used in this study. This treatment has been accepted in the study of Erkey and Akgerman [28]. However, in the work

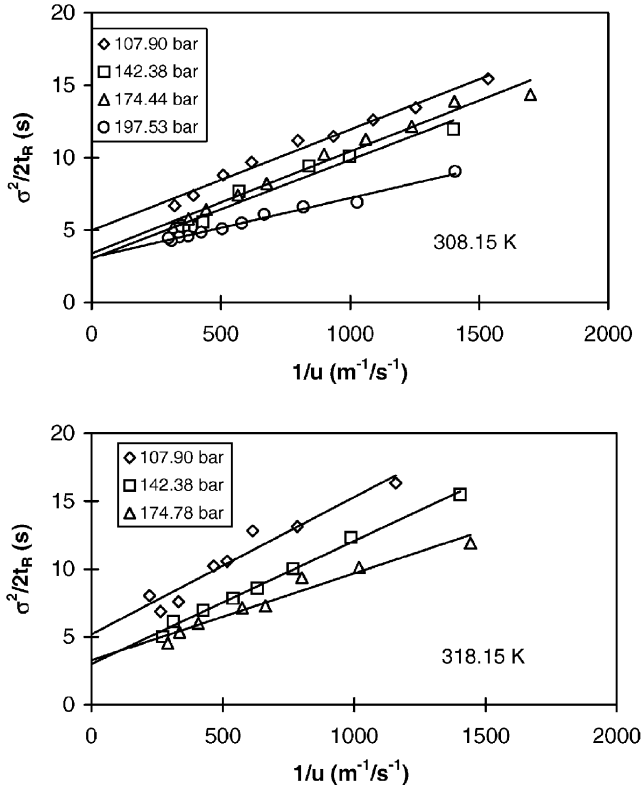

Fig. 9. Relation of $\sigma^2/2t_R$ with the reciprocal velocity ($1/u$) for toluene.

Table 3
Kinetic properties of two solutes in silica gel/CO_2

T (K)	P (bar)	ρ (g/cm^3)	Pe	D_e (m^2/s, $\times 10^{10}$)	D_e/D_m
1,4-Dichlorobenzene					
298.15	176.9	0.8988	0.2164	8.680	0.1111
	142.4	0.8699	0.2326	8.812	0.1026
	107.9	0.8299	0.1906	10.93	0.1135
	74.46	0.7600	0.1181	14.34	0.1342
308.15	174.4	0.8434	0.1897	9.480	0.1047
	142.4	0.8054	0.1994	10.74	0.1126
	107.9	0.7390	0.1716	16.21	0.1484
	82.74	0.5697	0.2327	12.15	0.08675
318.15	174.9	0.7829	0.2315	12.97	0.1124
	142.4	0.7270	0.2317	14.37	0.1140
	107.9	0.5888	0.2121	23.00	0.1389
Average					0.1163
Toluene					
308.15	197.5	0.8641	0.1748	7.341	0.08210
	174.4	0.8431	0.2637	8.446	0.09320
	142.4	0.8054	0.1980	11.42	0.1197
	107.9	0.7390	0.2381	9.293	0.08510
318.15	174.9	0.7829	0.2299	12.01	0.1041
	142.4	0.7270	0.1842	16.09	0.1307
	107.9	0.5888	0.2493	16.18	0.09807
Average					0.1019

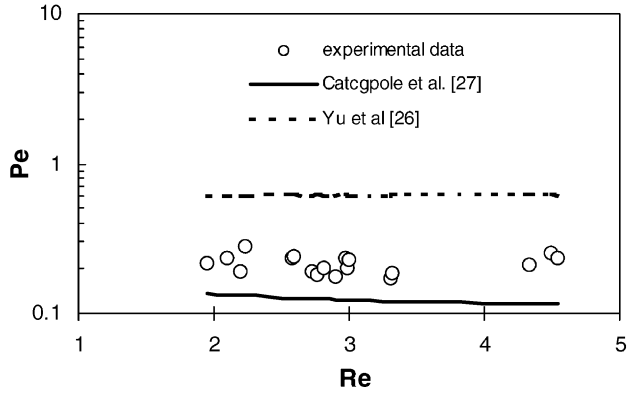

Fig. 10. Relationship between the Peclet number and the Reynolds number.

of Lee et al. [14], the assumption that the axial dispersion coefficient was independent of the flow rate is applied, but it failed to describe the experimental data in our work.

The variation of the Peclet number (Pe) with temperature and density was shown in Fig. 11. Temperature and density have relatively less effect on Pe in our experimental conditions. The axial dispersion in a packed bed may be a combination of the effects of convection and molecular diffusion. If controlled by molecular diffusion, the axial dispersion will reduce with pressure increasing and temperature decreasing. In contrast, it will increase with pressure if the convection is extremely important. The measured results suggest that neither molecular diffusion nor convection be the controlling factor for the axial dispersion process, thus both contributions may exist under the experimental conditions in this work.

4.6. Intraparticle diffusion

According to Eq. (8), the intercepts of the plots in Figs. 8 and 9 are related to a combination of the adsorption rate constant (k_{ad}), the external mass transfer coefficient (k_f), and the effective diffusivity (D_e). In this study, the contribution of the adsorption rate constant was neglected at all experi-

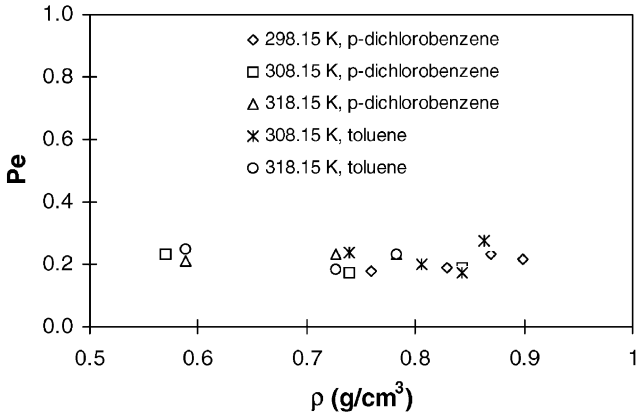

Fig. 11. Dependence of the Peclet number with temperature and density in dense CO_2.

mental conditions. The external mass transfer coefficient (k_f) was estimated by the following correlation equation [33].

$$\frac{d_p k_f}{D_m} = 2.0 + 1.1\left(\frac{\eta}{\rho D_m}\right)^{1/3}\left(\frac{d_p u \rho}{\eta}\right)^{0.6} \quad (19)$$

where η is the viscosity of CO_2, which was calculated by a reference equation [34]. D_m is the molecular diffusion coefficients of the two solutes in dense CO_2. For toluene it is from the reference [35], and for 1,4-dichlorobenzene it is determined by the work of Fu et al. [36].

The influence of fluid velocity on the mass transfer coefficients at low *Re* was neglected, which is due to the assumption that the change of *Re* has little influence on the mass transfer coefficient [14]. So the average *Re* at each experimental condition was used to calculate the mass transfer coefficient. Table 3 gives the effective intraparticle diffusion coefficients (D_e) at each experimental condition, together with the ratio of D_e/D_m. As expected, the effective diffusivity within the porous solid is lower than the bulk diffusivity. The ratio, D_e/D_m, ranged approximately from 0.09 to 0.14 for 1,4-dichlorobenzene and 0.08 to 0.13 for toluene.

Diffusion in a porous solid may occur by one or more of three mechanisms: pore (bulk), Knudsen, and surface diffusions. In the absence of surface diffusion, which is less possible due to a lower solute concentration in the fluid, if the pores are large and the fluid is relatively dense, the pore diffusion should be the main diffusion mechanism. Consequently, it may be expected that the effective intraparticle diffusivities should show a similar temperature and pressure dependence as the bulk diffusivities. The measured data of the effective diffusivity in Table 3 reflect a reasonable trend with temperature and pressure, though there is an unusual decrease with pressure in the experimental data near the critical pressure of CO_2 at 308.15 K, which may be caused by the critical effect [37] or the experimental errors.

The effective diffusivity in porous solid can be described by the expression [38]

$$D_e = \frac{D_m \varepsilon_p}{\tau} F(\lambda) \quad (20)$$

where τ is the tortuosity factor of porous solid. $F(\lambda)(= 1-\lambda)^4)$ is a factor that accounts for the restriction diffusion. The parameter λ is the ratio of molecular diameter to pore diameter. The molecular diameter of 1,4-dichlorobenzene was estimated as 0.60 nm using a group contribution method [39]. The average value of D_e/D_m in Table 3 can be used to calculate the tortuosity factor τ. A value of 2.9 is obtained for the tortuosity factor. For toluene the calculated value of τ is 3.2. The values of τ are reasonable considering that the reported values in the literatures range from 2 to 6 [28,38]. So Eq. (20) is applicable to estimate the effective diffusivity within porous solids in supercritical fluids.

The contribution of each rate process to the second central moment was evaluated by using the estimated parameters. Fig. 12 shows the individual contribution of the axial dispersion, intraparticle diffusion, and the external mass transfer as a function of *Re* at a typical experimental condition, 308.15 K and 142.38 bar, for 1,4-dichlorobenzene. The contribution of the intraparticle diffusion becomes more important with the increase of *Re*, while the axial dispersion contribution decreases. It was also observed that the contribution of the mass transfer was relatively minor, <10%. This means that the estimation method of k_f has little effect upon the evaluation of the effective intraparticle diffusivity. For example, the external mass transfer resistance has been neglected in the previous study of Erkey and Akgerman [28].

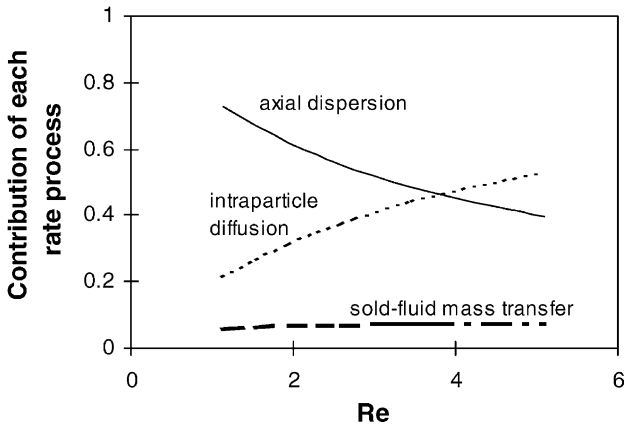

Fig. 12. Contribution of each rate process to peak broadening.

5. Conclusions

The impulse chromatographic technique has been applied to determine the equilibrium and kinetics parameters for 1,4-dichlorobenzene and toluene in the silica gel/dense CO_2 system. The first and second moments of the chromatographic peaks were analyzed by the series fitting method, which overcomes the shortcoming of traditional numerical integration method and can be used to very skewed peaks. The adsorption equilibrium constants of the two solutes on the silica gel were determined in dense CO_2. The two solutes possess an equivalent affinity on the silica gel adsorbent. The adsorption equilibrium constant increases with temperature and decreases with pressure under the experimental conditions. The fluid density is found to be the main controlling factor determining the adsorption equilibrium constant.

The partial molar volumes and partial molar enthalpies for 1,4-dichlorobenzene in the supercritical CO_2 were evaluated using the adsorption equilibrium constant measured. Very large and negative values for the two partial molar properties were observed near the critical point of CO_2. A comparison has been made through calculating the two partial molar properties from the PR equation of state.

The Peclet number, associated with the axial dispersion coefficient, and the intraparticle effective diffusivity were obtained from the second moments of the response peak. The axial dispersion in this study is similar with the disper-

sion behavior in liquid phase. The dependence of the Peclet number on temperature and pressure is relatively small. The pore diffusion is the main mechanism of intraparticle diffusion in our experimental conditions.

References

[1] E. Kiran, J.M.H. Levelt Sengers (Eds.), Supercritical Fluids Fundamentals for Application, Kluwer Academic Publisher, Dordrecht, 1994.
[2] M.A. McHugh, V.J. Krukonis, Supercritical Fluid Extraction, Principles and Practices, 2nd ed., Butterworth-Heinemann, 1994.
[3] J. Benkhedda, J.-N. Jaubert, D. Barth, et al., Sep. Sci. Technol. 36 (2001) 2197.
[4] J.R. Conder, C.L. Young, Physicochemical Measurement by Gas Chromatography, New York, 1979.
[5] N. Wakao, S. Kaguei, Heat and Mass Transfer in Packed Beds, Gordon and Breach, New York, 1982.
[6] J.-J. Shim, K.P. Johnston, J. Phys. Chem. 95 (1991) 353.
[7] A. Akgerman, G. Madras, in: E. Kiran, J.M.H. Levelt Sengers (Eds.), Supercritical Fluids Fundamental for Application, Kluwer Academic Publisher, Dordrecht, 1994.
[8] P. Schneider, J. Smith, AIChE J. 14 (1968) 762.
[9] R.L. Cerro, J.M. Smith, AIChE J. 16 (1970) 1034.
[10] C.S. Tan, D.C. Liou, Ind. Eng. Chem. Res. 28 (1989) 1246.
[11] F. Dondi, A. Betti, G. Blo, C. Blghi, Anal. Chem. 53 (1981) 496.
[12] K.R. Harris, J. Sol. Chem. 20 (1991) 595.
[13] M. Abramowitz, I. Segum, Handbook of Mathematical Functions with Formulas, Graphs and Mathematical Tables, Dover, New York, 1965.
[14] C.-H. Lee, S.H. Beyon, C. Holder, J. Chem. Eng. Jpn. 29 (4) (1996) 683.
[15] J.W. King, Supercritical fluids, in: T.G. Squires, M.E. Paulaitis (Eds.), ACS Symposium Series, Washington, DC, 1987.
[16] M. Sato, M. Goto, A. Kodama, T. Hirose, Sep. Sci. Technol. 33 (9) (1998) 1283.
[17] M. Goto, M. Sato, S. Kawajiri, T. Hirose, Sep. Sci. Technol. 31 (12) (1996) 1649.
[18] IUPAC, in: Angus, et al. (Eds.), Pergamon Press, New York, 1976.
[19] J.F. Brennecke, C.A. Eckert, AIChE J. 35 (1989) 1409.
[20] C.R. Yonker, R.W. Gale, R.D. Smith, J. Phys. Chem. 91 (1987) 3333.
[21] D. Peng, D.B. Robinson, Ind. Eng. Chem. Fundam. 15 (1976) 59.
[22] J. Puiggene, M.A. Larrayoz, F. Deccusens, Chem. Eng. Sci. 52 (2) (1997) 195.
[23] P.G. Debenedetti, Chem. Eng. Sci. 52 (1997) 195.
[24] F.D. Kelley, E.H. Chimowitz, AIChE J. 36 (1990) 1163.
[25] R.C. Reid, J.M. Prausnitz, B.E. Poling, The Properties of Gases and Liquids, 4th ed., McGraw-Hill, New York, 1987.
[26] D. Yu, K. Jackson, T.C. Harmon, Chem. Eng. Sci. 54 (1999) 356.
[27] O.J. Catchpole, R. Bernig, M.B. King, Ind. Eng. Chem. Res. 35 (1996) 824.
[28] C. Erkey, A. Akgerman, AIChE J. 36 (1990) 1715.
[29] D.J. Gunn, Chem. Eng. Sci. 42 (1987) 363.
[30] C.G. Hill, Chemical Engineering Kinetics and Reactor Design, Wiley, New York, 1979.
[31] A.W. Liles, C.J. Geankoplis, AIChE J. 6 (1960) 591.
[32] C.C. Fu, M.S.P. Ramesh, H.W. Haynes, AIChE J. 32 (1986) 1848.
[33] N. Wakao, T. Funazkri, Chem. Eng. Sci. 33 (1978) 1375.
[34] V. Vescovic, W.A. Wakeham, G.A. Olchowy, J.V. Sengers, J.T.R. Watson, J. Millat, J. Phys. Chem. Ref. Data 19 (1990) 763.
[35] J.J. Suarez, J.L. Bueno, I. Medina, Chem. Eng. Sci. 48 (1993) 2419.
[36] H. Fu, L.A. Coelho, M.A. Matthews, J. Supercrit. Fluids 18 (2000) 141.
[37] X.N. Yang, L.A.F. Coelho, M.A. Matthews, Ind. Eng. Chem. Res. 39 (2000) 3059.
[38] C.N. Satterfield, C.K. Colton, W.H. Pitcher, AIChE J. 19 (1973) 268.
[39] J.T. Edward, J. Chem. Edu. 47 (1970) 261.